



SIEMENS

Ingenuity for life

Siemens Digital Industries Software

Using simulation to predict cavitating flow

Leveraging CFD software to conduct accurate, full-scale simulation of propellers

Executive summary

This paper examines the challenges of simulating cavitating flows, especially flows around propellers. First the sources of various errors are highlighted: the accuracy of geometry, grid quality and fineness, turbulence modeling and cavitation modeling. The interaction between errors from different sources is also discussed. The importance of turbulence in the flow upstream of propeller and the difficulty of accounting for it is described next. Special attention is paid to the prediction of tip-vortex cavitation and scale effects. Results from Simcenter™ STAR-CCM+™ software simulations are compared to experimental data from SVA Potsdam GmbH, an independent shipbuilding research institute, except for the full-scale analysis of flow around hull, propeller and rudder, for which no experimental data is available.

Milovan Perić
Institute of Ship Technology,
Ocean Engineering and Transport Systems
University of Duisburg-Essen

Contents

Introduction.....	3
1. Errors to consider in simulation	4
2. Cavitation models in Simcenter STAR-CCM+	5
3. Two-dimensional approximation	6
4. Accuracy of geometry	7
5. Accounting for turbulence	9
6. Incipient cavitation	11
7. Tip-vortex cavitation.....	12
8. Solution-adaptive grid refinement.....	15
9. Scale effects.....	16
Conclusion	17
References	17

Introduction

Cavitation is an important phenomenon that occurs in many flows, especially in rotating machinery (turbines, pumps, propellers) and around valves. The main cause is flow acceleration, leading to pressure falling below saturation level for a given temperature. A typical example of such flow acceleration is the leading edge of a propeller; the lowest pressure is usually found on the suction side close to the leading edge. However, flow acceleration can also happen due to wall vibration, especially at high frequencies and/or amplitudes of motion. In most cavitating flows, a relatively small amount of liquid evaporates compared to the total flow rate. The heat needed for the phase change is taken from the surrounding liquid, but due to the small amount of liquid that evaporates, temperature in the liquid is usually assumed to stay constant.

The phase change happens at the interface between the liquid and gas phases. A perfectly purified liquid without any solid particles or bubbles of non-condensable gases can sustain large tensile stresses caused by negative absolute pressure. The lowest measured pressure in water we are aware of before cavitation started is –280 bar.¹ However, liquids encountered in engineering and nature are far from pure; they contain seed bubbles (either bubbles of non-condensable gases like air or gas inclusions in crevices on solid particles) from which phase change can start, leading to larger cavitation bubbles. In some flow zones where bubble residence times are relatively long (for example, in recirculation zones), bubbles can grow so large that they merge and form a vapor sheet or cloud.

Cavitation not only adversely affects the performance of the flow device – it also leads to vibration, noise and erosion and could even cause structural damage. It is therefore important to be able to predict with acceptable accuracy whether cavitation takes place at a particular operating point and what kind of cavitation it is in order to take mitigating measures.

Nowadays computational methods are regularly used to investigate such flow features. Computational fluid dynamics (CFD) plays a major role in the development of new products and their optimization and is part of a virtual or comprehensive digital twin approach to product development. Complex geometries can be imported

directly from computer-aided design (CAD) tools and the computational grid is then generated automatically and can be locally refined where higher resolution is required to capture features of interest. The Navier-Stokes equations are then solved on this grid to predict fluid behavior.

Most engineering flows in which cavitation occurs are turbulent; this is especially true for the flow around a ship and propeller at full scale. Because we cannot afford to resolve all turbulent fluctuations in space and time, we cannot use pure Navier-Stokes equations to simulate such flows. When computing the flow around a ship hull, with or without including the propeller, we instead use Reynolds-averaged Navier-Stokes (RANS) equations where the effects of turbulence are accounted for by using one of many available turbulence models. The most widely used models are of the eddy-viscosity type; they determine the so-called turbulent viscosity by solving two additional equations. Turbulent viscosity (which may vary by several orders of magnitude within the solution domain) is then added to the fluid viscosity. For more details on RANS-based simulation approaches, see books on this subject and references therein.^{2,3,4,5}

When the Reynolds number is moderate, such as when simulating the flow around a model scale propeller, one can use methods based on large-eddy simulation (LES), in which filtered Navier-Stokes equations are solved. Larger scales from the turbulence spectrum are resolved and the smaller, more universal scales are modeled. One needs to use finer grids and smaller time steps than in the RANS approach, which makes this method more computationally intensive. The modeling of sub-grid-scale turbulence is usually achieved using algebraic models, like the one from Smagorinsky.⁶

Cavitation and multiphase flows are other features of engineering flows that cannot be fully resolved. They are also modeled, meaning the equations solved in CFD are not exact. Therefore, one must bear in mind that CFD delivers only *approximate solutions* that always contain errors from different sources. In this white paper we consider important aspects of cavitation simulations for ship propellers and assess the relative impact of potential errors on simulation accuracy and how the errors can be reduced.

1. Errors to consider in simulation

Iteration errors occur because we solve discretized governing equations iteratively and have to stop iterations at some stage. They are relatively easy to control by monitoring residuals and quantities of particular interest, such as thrust and torque on a propeller. When the residuals are reduced by approximately 4 orders of magnitude, we can expect that variable values are not changing on the three most significant digits, which is usually enough; that corresponds to iteration errors on the order of 0.1 percent or less.

Discretization errors depend on the choice of approximations used in different discretization steps. These can include approximation of surface, volume and time integrals; interpolation of the solution to locations other than computational points; approximation of gradients, etc. They also depend on the properties of the computational grid. For given selections, discretization errors can only be reduced by refining the grid. However, comparing results from a series of systematically refined grids may be deceiving if the original grid design is unsuitable to resolve all the relevant flow features. This will be examined in more detail later.

Modeling errors are usually the largest and most difficult to estimate. There are many possible sources of such errors, the major ones being:

- Turbulence model
- Cavitation model
- Geometry of the solution domain not being the same as in reality
- Boundary conditions not corresponding to reality
- Incorrect fluid properties

The first three causes of modeling errors will be discussed in more detail in the following sections.

What makes assessing the accuracy of numerical simulations difficult is that errors from different sources interact with each other: They may partially cancel out or augment each other, depending on their sign and magnitude. In order to minimize such effects, it is important to ensure iteration errors are at least an order of magnitude lower than discretization errors, and that discretization errors are at least an order of magnitude lower than modeling errors.

The rest of this white paper considers the challenges in simulation of cavitating flows. In the following section the two cavitation models available in Simcenter STAR-CCM+, which is part of the Xcelerator™ portfolio, the comprehensive and integrated portfolio of software and services from Siemens Digital Industries Software, are briefly described, followed by a discussion of the suitability of two-dimensional approximations for simulations of cavitating flows. Next the accuracy of the solution domain geometry representation in simulation is discussed. This is followed by a section devoted to the effects of the turbulence modeling approach. Section 6 is devoted to incipient cavitation and section 7 to the prediction of tip-vortex cavitation. In section 8 the advantages of solution-adaptive grid refinement are discussed using growth and collapse of a single bubble near wall as an example. This is followed by an assessment of scale effects and concluding remarks.

2. Cavitation models in Simcenter STAR-CCM+

Most cavitation models are based on the assumption that liquid contains seeds from which cavitation bubbles can grow when the pressure becomes lower than saturation pressure. The number of seeds per cubic meter of liquid and their initial diameter are parameters of the model, by which the purity of the liquid can be taken into account. The modeling is based on the homogeneous two-phase flow assumption: Equations of motion are solved for a single effective fluid, and the distribution of vapor and liquid phase is determined by solving an additional equation for the vapor volume fraction. This is similar to the volume of fluid (VOF) method for free-surface flows, but with two distinctions. First, for cavitation the equation for vapor volume fraction contains a source term, which governs the growth and collapse of cavitation bubbles. Secondly, vapor volume fraction in cavitating flows can vary smoothly between 0 and 1, while in free-surface flows a sharp interface between the phases is assumed. The source term is based on estimated bubble growth or collapse rates.

Simcenter STAR-CCM+ is a multiphysics CFD software from Siemens. It contains two cavitation models that differ in how they determine bubble growth or collapse rate:

- The full Rayleigh-Plesset model, in which the bubble growth rate is determined by solving the Rayleigh-Plesset equation in its complete form

$$R \frac{d^2R}{dt^2} + \frac{3}{2} \left(\frac{dR}{dt} \right)^2 = \frac{p_s - p}{\rho_l} - \frac{2\sigma}{\rho_l R} - 4 \frac{\mu_l}{\rho_l R} \frac{dR}{dt}$$

Saturation pressure Surrounding pressure Surface tension Liquid viscosity

Bubble radius Liquid density

- The Schnerr-Sauer model,⁷ in which the bubble growth rate is determined from a simplified expression containing only the framed part of the above equation. When the pressure in the surrounding liquid is higher than the saturation pressure, a square root is taken from the absolute value of pressure difference and a minus sign is added to the result. Although this is mathematically incorrect, it is a plausible approximation that still leads to acceptable solutions.

The full Rayleigh-Plesset model requires smaller time steps and thus increases the computational cost compared to the simpler Schnerr-Sauer model. The latter is robust and in most engineering applications leads to solutions of acceptable accuracy, as will be shown in the following sections. The model has often been blamed for errors that come from other sources.

Users can also calibrate the Schnerr-Sauer model for a particular application by using two functions that multiply the positive (bubble growth) and negative (bubble collapse) source term in the vapor volume fraction equation.

3. Two-dimensional approximation

When the geometry is axisymmetric or does not change in the spanwise direction, a 2D approximation is often used to reduce the computational effort. This is usually justifiable if the flow is statistically steady. However, cavitating flows are often strongly unsteady. An example of this is cloud cavitation, which is characterized by periodic growth and detachment of the vapor cloud. Unsteady flows are usually strongly 3D. By constraining the velocity field to two dimensions in a 2D simulation, many features of cavitating flows observed in experiments cannot be adequately simulated. Good examples of this are cloud cavitation on propellers and rudders.

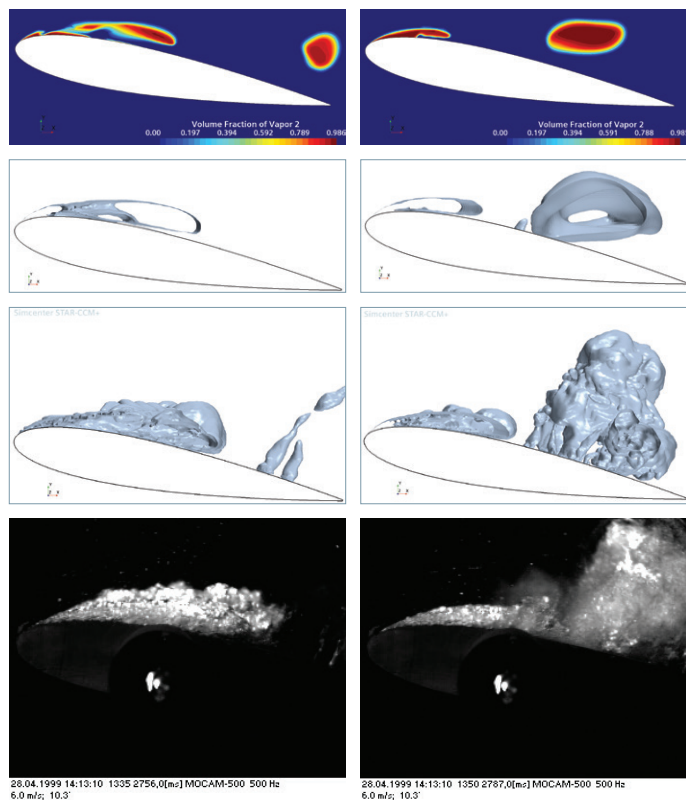


Figure 1. Cavitation on a NACA0015 hydrofoil, spanned between side walls of a cavitation tunnel: distribution of vapor volume fraction in 2D unsteady RANS simulation (first row), side view of iso-surfaces of vapor volume fraction 0.05 from 3D unsteady RANS simulation (second row) and from LES simulation (third row) and side view of cavitation bubbles in an experiment performed at HSVA Hamburg (bottom row).

Figure 1 shows representative pictures from 2D and 3D RANS simulations and an LES simulation, performed with Simcenter STAR-CCM+ using the Schnerr-Sauer cavitation model, for the flow around a NACA0015 hydrofoil at a 10.3-degree angle of attack. The chord length of the foil was 0.2 meters (m), flow speed was 6 meters per second (m/s), the absolute pressure in the cavitation tunnel was 32,900 Pascal (Pa) and the saturation pressure for water at given temperature was 2,300 Pa (cavitation number 1.7). For comparison, results are also shown from the experiment performed at HSVA Hamburg.⁸ In the 2D simulation, the buildup of a large cavitation zone and its detachment are predicted, but the features of the flow are substantially different from those observed in experiment. A 3D simulation with a RANS model (here the default k- ϵ model was used) produces a significant improvement in solution quality. However, only the LES analysis leads to solutions that exhibit similar flow features to those seen in the experiment, even when the simplest cavitation model (Schnerr-Sauer) is used. Similar conclusions regarding comparisons of RANS and LES solutions were drawn in a study by Muzaferija et al.,⁹ where the benefit of using a more advanced cavitation model (Full Rayleigh-Plesset) is also documented.

4. Accuracy of geometry

In numerical simulations of fluid flow, the geometry of the solution domain is taken from a CAD model. In a CAD model of a propeller, all blades are identical and the circumferential distance between them is the same. However, the geometry of a manufactured propeller used in model tests or on the real vessel usually differs from CAD. One reason is the manufacturing tolerance: the casting process, followed by the manual final surface preparation and polishing. Model-scale propellers used for physical testing in towing tanks typically have a diameter of between 0.2 and 0.25 m. This makes it particularly difficult to achieve the blade shape specified in the CAD model. The International Towing Tank Conference (ITTC) specifies in its guidelines that a model-scale propeller for tests should be manufactured with 0.1 millimeter (mm) tolerance, and 0.05 mm for the leading end trailing edges.

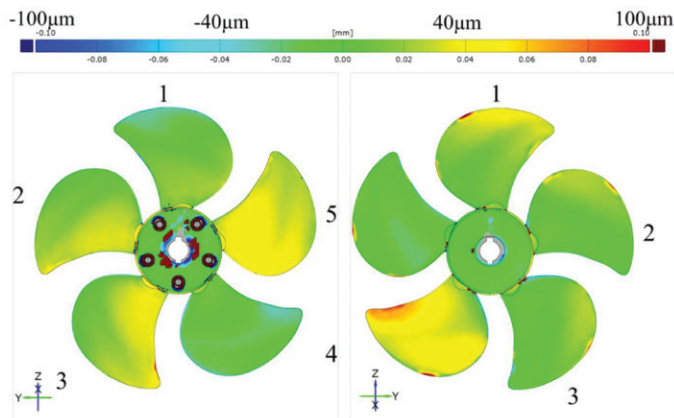


Figure 2. Deviation of the manufactured geometry from the CAD model for the Potsdam Propeller Test Case.

In order to assess the differences between a manufactured propeller and the CAD model, SVA Potsdam¹⁰ performed detailed measurements of the built geometry of two samples of their Potsdam Propeller Test Case (PPTC). Figure 2 shows the deviations of both suction and pressure sides from the CAD model for all five blades. Although the deviations are clearly within the ITTC recommendation, it is also obvious that each blade

is different. For example, blade 5 is almost identical to the CAD geometry on the suction side, but around 0.05 mm off on the pressure side. The same is true for blade 4, but the pressure side is perfect and the suction side is off by up to 0.1 mm.

Although the optical scanning of suction and pressure side of propeller blades is relatively easy, measuring the shape of leading and trailing edges is difficult. Since 2016 SVA Potsdam has been able to make such measurements. They performed a detailed assessment of the leading edge geometry for two versions of the PPTC propeller (controllable pitch and fixed pitch), along the contour of constant radius $r = 0.7R$, where R is the propeller diameter. Figure 3 shows the contours of the two manufactured propellers, together with the contour taken from the CAD model. The CAD model geometry exhibits a pronounced "nose" at the leading edge, with a small radius of curvature, followed with short sections on both sides, which are almost straight lines at the end of which larger radii of curvature connect these lines to the blade contour on pressure and suction sides. In contrast, both manufactured profiles have a smoothly varying curvature of the leading edge, which is significantly different from the CAD shape, although within the ITTC tolerance. These slight differences in geometry can have significant influences on the measured propeller properties. Both the stagnation line (along which the flow splits to suction and pressure side streams) and the possible tendency to flow separation and cavitation may be significantly influenced by the difference between the CAD shape and manufactured shape.

Figure 3 also includes a plot of grid and pressure distribution from a simulation of flow around the PPTC propeller. In this simulation the thickness of the first cell next to the wall was 0.005 mm, which means the dimensionless distance of the first computational point from wall is close to $y^+ = 1$. This is required to resolve the viscous sublayer; for example, when using a low-Re wall treatment in RANS computations, or when using an LES approach to turbulence modeling. By comparing the two plots in figure 3 it is obvious that several near-wall prism layers in the computational grid fall within the difference between the CAD profile and the manufac-

tured profile. Also, the blade is thicker in both manufactured models than in the CAD model. In the middle of the blade part shown in figure 3, the thickness difference is about 9 percent.

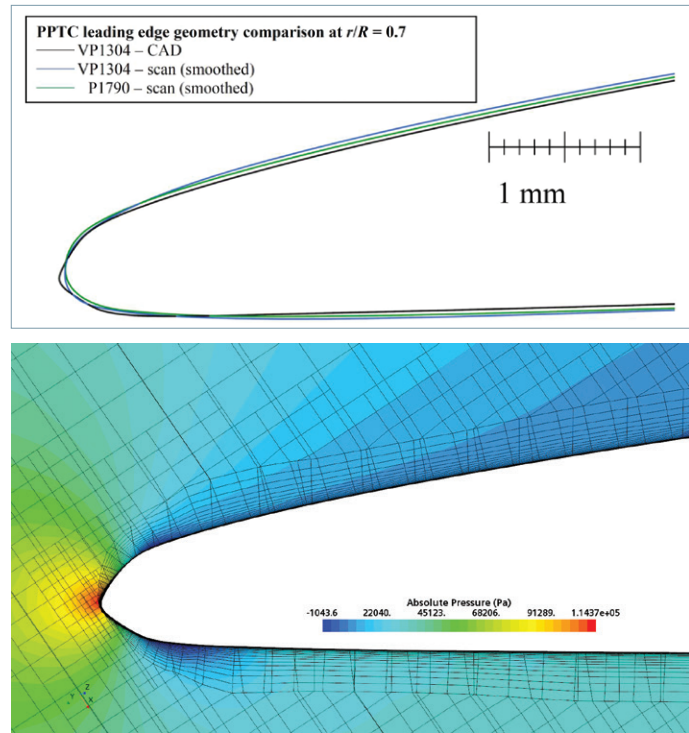


Figure 3. Deviation of the two manufactured blade profiles at $r/R = 0.7$ from CAD (upper) and the cut through numerical grid with pressure distribution around the CAD profile (lower).

Unfortunately, there is no full-scale CAD of the manufactured geometry, which could be used to generate the grid for flow simulation in a domain bounded by the built geometry. Only by comparing solutions obtained using CAD geometry and built geometry would it be possible to reliably assess the significance of the observed discrepancy between manufactured propellers and the CAD model. Jin et al.¹¹ studied the effects of simplified leading-edge defects on the 2D flow around an airfoil and found that defects within the allowed tolerance can significantly affect cavitation inception. It would also be important to assess the effects of the difference between individual propeller blades, but this too requires a CAD model of the built geometry. We hope that such data will become available in the near future.

Even when we have the correct geometry as input, the generated grid may not produce an accurate

representation of the CAD geometry. It is easy to misrepresent the geometry if the grid is not sufficiently refined locally, especially when the CAD model contains parts with a small curvature radius. An example is shown in figure 4, a longitudinal cut through the polyhedral grid around the PPTC propeller and a surface view of the leading edge for two grids. In one grid the leading-edge zone is locally refined so the curvature of the leading edge is relatively accurately represented, while in the other grid no special measures were taken to refine the grid where curvature is high. Further away from the leading edge, the two grids have cells of a similar size.

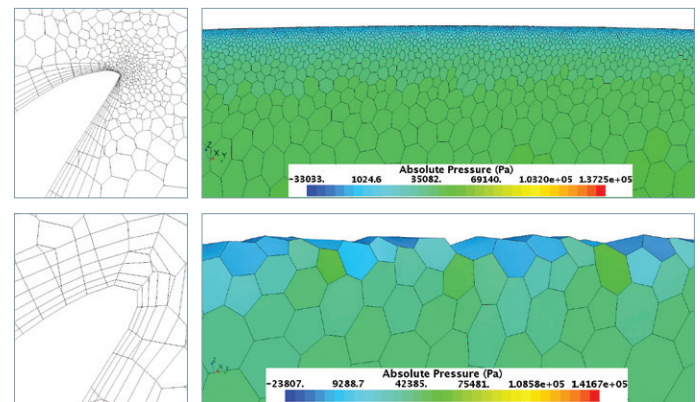


Figure 4. Representation of leading-edge geometry by the computational grid in a longitudinal section through propeller blade (left) and in a view of the blade from the suction side (right), from a locally refined grid with minimum cell size 0.011mm (upper) and a coarse grid with minimum cell size 0.176 mm (lower).

As can be seen in figure 4, the coarse grid representation of the leading edge geometry is far from the CAD geometry. The curvature is not resolved and the leading edge is rough. Obviously, the two grids represent two different geometries of the propeller blade leading edge. Thus, when we compare CFD solutions from these two grids, we see a difference that is not only due to different cell size in critical zones, but also due to the different shapes of propeller blade.

In this example, simulations were performed for a single blade with periodic conditions in the circumferential direction. The coarse grid had 930,649 cells and the grid with local refinement along the leading edge had 3,309,770 cells. Having observed the difference in leading-edge resolution one would expect a significant difference in the solutions obtained with the two grids. The blunt and rough form of the leading edge from the coarse grid suggests the solution should be significantly

in error. However, comparing thrust and torque computed on the two grids leads to a surprising outcome: the results do not differ much! Table 1 presents the thrust and torque for the blade computed on the two grids and the measured values from experiment.¹²

	Experiment	Coarse grid	Locally refined grid
Thrust	181.74 N	183.4 N (+0.91%)	182.95 N (+0.67%)
Torque	11.796 Nm	12.13 Nm (+2.83%)	12.06 Nm (+2.24%)

Table 1. Comparison of results from two grids with experimental data from SVA Potsdam.

The difference between solutions obtained on the two grids is much smaller than the difference between either solution and experimental data. One may ask: how is that possible? The answer lies in partial cancellation of errors. Because of the randomness of leading edge "roughness" due to a too coarse grid, local errors in force along the leading edge vary in amplitude and sign. When the forces are integrated over the entire blade, these positive and negative errors partially cancel each other out. However, one cannot expect that such a partial cancellation will happen for every operating point or for every propeller. For reliable solutions, especially when simulating cavitation, one needs to design the grid such that important geometry features are adequately resolved.

5. Accounting for turbulence

Certain flow phenomena cannot be captured well when a RANS approach is used. One example is the beginning of suction-side cavitation on propeller blades. Experimental observations at SVA Potsdam show that under particular conditions cavitation bubbles appear on the downstream half of the suction side, as shown in the sketch in figure 5. RANS simulation does not produce such cavitation even when a very fine grid is used. In the example shown here a very fine grid of 29 million cells for a single blade with periodic conditions in the circumferential direction was used. Using an LES model and the same grid, cavitation bubbles do appear in the zone indicated by experimental observations. Because the same grid and cavitation model are used in both RANS and LES simulations, the difference is obviously due to the turbulence modeling approach alone.

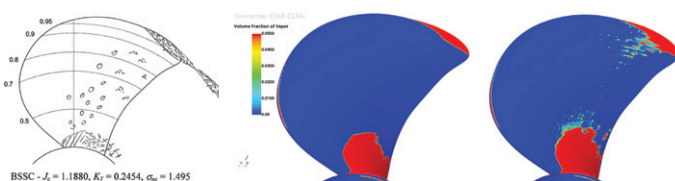


Figure 5. Cavitation on blade suction side: observation in experiment¹³ (left), RANS solution (middle) and an instantaneous picture from the LES solution (right).

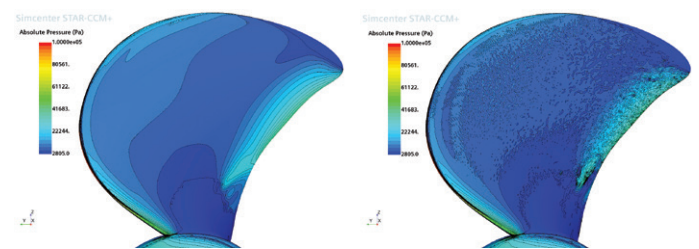


Figure 6. Distribution of instantaneous pressure on the suction side of the propeller blade from a RANS solution (left) and from a LES solution (right) for conditions from figure 5.

Figure 6 explains why the RANS approach cannot predict cavitation on the suction side. The mean pressure is below saturation level only in the zones where the tip-vortex cavitation and blade-root cavitation were visible in figure 5. Over the rest of the suction side blade surface, the pressure is above saturation level and the cavitation does not happen. Even though the RANS simulation was performed in an unsteady mode using an SST k- ω turbulence model,⁵ the solution was practically steady except at the edges of the tip-vortex and blade-root cavitation zones.

In the LES simulation, turbulent fluctuations of velocity and pressure are resolved up to the grid scale. This is clearly seen in figure 6 (right), which shows that pressure not only fluctuates over the blade surface, but that local low-pressure zones are present. These small low-pressure zones are created when the fluctuating (fluttering) boundary layer tends to move away from the blade surface. In an animation one can see how the local low-pressure zones appear, move over some distance and then disappear. The same happens to vapor bubbles: They are created when the pressure falls below saturation pressure, and they move until the pressure rises again above saturation level, leading to bubble collapse. Therefore, this kind of bubbly cavitation can only be predicted by turbulence modeling approaches that resolve the velocity and pressure fluctuations. RANS methods do not fall into this category. Note the sketch in figure 5 shows the experimental observation of bubble appearance over a longer period of time while the picture from the LES simulation shows an instantaneous situation, which changes with time.

Figure 7 shows the pressure distribution on a longitudinal section through the blade and propeller hub, which is computed on the same grid as before and compares RANS and LES results. The main features are similar, but there are also important differences:

- The LES solution shows turbulent fluctuations behind the hub and near the blade wall where the contours from the RANS simulation are smooth
- The pressure in the tip-vortex core is much lower in LES than in RANS results
- The low pressure zone on the pressure side near the blade root is larger in the LES than in the RANS solution

These differences are important as they form part of the conditions for hub and tip-vortex cavitation. This will be discussed later.

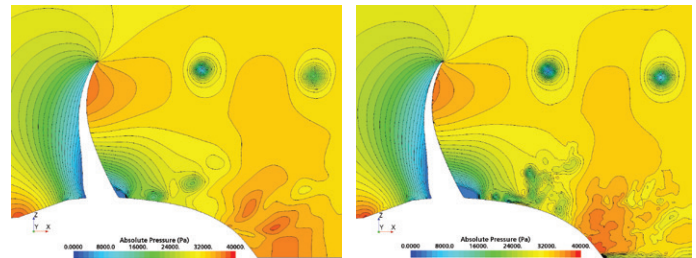


Figure 7. Distribution of instantaneous pressure in the longitudinal section through a propeller blade from a RANS solution (left) and an LES solution (right) for conditions from figure 5.

When studying the flow around a propeller mounted on a vessel, the velocity field approaching the propeller is highly inhomogeneous. This means during its rotation a propeller blade encounters different magnitudes and directions of velocity and different turbulence levels. In order to accurately predict cavitation and especially hydro-acoustics, it is important to correctly account for the turbulence in the incoming flow, as this affects the flow around the propeller blades. Unfortunately, applying LES simulation to the flow around the entire hull and all appendages is not possible in practical applications, not even at model scale. Instead, one could do embedded LES solutions of the flow around the propeller. The turbulent fluctuations in the upstream flow are reconstructed from the surrounding RANS solution of the flow around the hull. Such simulations are just emerging^{14,15} and more applications of this kind are expected in future.

6. Incipient cavitation

If the aim is to avoid cavitation, it is not necessary to use two-phase flow analysis with a particular cavitation model. Instead, it is only necessary to determine under which conditions cavitation begins. From a single-phase analysis, one can recognize whether cavitation will be taking place or not by examining pressure distribution in the solution domain. If pressure falls below saturation level in any location, then cavitation will be taking place. However, it may be difficult to determine whether cavitation is significant or not: If pressure is only slightly below saturation level in a very small volume, that may not affect the flow and propeller performance to a critical extent. Criteria to determine the cavitation inception are also not well defined in physical experiments: usually, an engineer observing the flow needs to decide when to classify the flow as being affected by incipient cavitation.

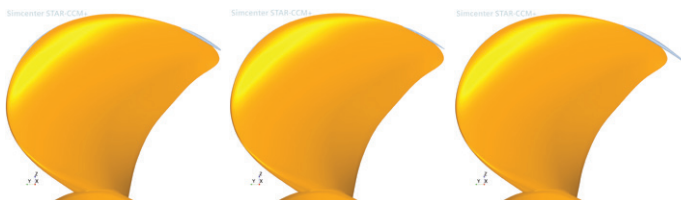


Figure 8. Simulation of incipient cavitation around propeller: iso-surface of 5 percent vapor volume fraction (left) and iso-surface of saturation pressure (middle) from a two-phase computation using cavitation model, and iso-surface of saturation pressure from a single-phase computation without cavitation model (right).

Figure 8 shows iso-surfaces of saturation pressure (2873 Pa absolute) from a two-phase simulation of flow around a propeller using the Schnerr-Sauer cavitation model, and from a single-phase flow without a cavitation model, compared with iso-surface of 5 percent vapor volume fraction from the two-phase simulation. When cavitation is not modeled (shown on the right), the zone of low pressure is larger than in the case of two-phase flow, and also somewhat larger than the zone in which vapor volume fraction is larger than 5 percent. The minimum value of absolute pressure is also significantly lower than in the case of two-phase flow, as shown in figure 9: -23902 Pa compared with 2732 Pa (141 Pa below saturation pressure).

Flow	Thrust (exp.)	Thrust (simulation)	Torque (exp.)	Torque (simulation)
Two-phase	218.28 N	216.50 N (-0.82%)	13.544 Nm	13.834 Nm (+2.14%)
Single-phase		216.05 N (-1.07%)		13.820 Nm (+2.04%)

Table 2. Comparison of solutions from a two-phase and a single-phase simulation of flow around propeller under incipient tip-vortex cavitation conditions with experimental data from SVA Potsdam (case no. 3, page 2.9).

In spite of the differences in these details between single-phase and two-phase simulations of flow with incipient cavitation, the integral quantities of engineering interest do not differ much, as can be seen in table 2. The predicted thrust from a single-phase simulation is only 0.25 percent lower than from a two-phase simulation, while the difference in torque is only 0.1 percent.

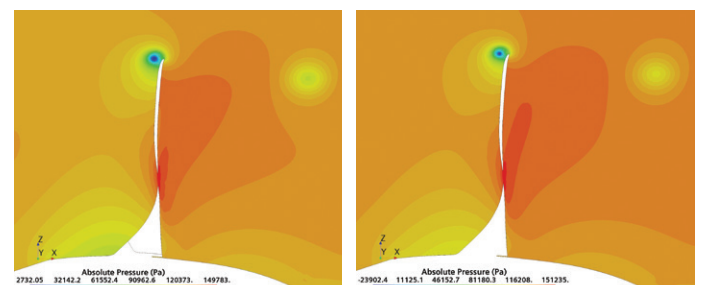


Figure 9. Pressure distribution in a section through propeller blade orthogonal to the iso-surfaces from figure 8, from a two-phase simulation (left) and from a single-phase simulation (right).

Single-phase prediction is only sufficient to determine the first occurrence of cavitation. In many cases cavitation occurs at more than one location in the flow, for example at blade leading edge, blade root, tip vortex and hub vortex. When that is the case, one has to use two-phase simulation to predict the propeller performance because cavitation does not start at the same time at all locations.

Note that negative absolute pressure in the liquid phase may occur even when a cavitation model is active in a two-phase flow simulation. Inside vortices and recirculation zones, where the residence time of vapor bubbles is long enough, pressure remains close to saturation pressure. However, in flow zones where flow acceleration is high and the residence time short, pressure in the liquid may become low, leading to high bubble growth rates but not necessarily a high vapor volume fraction. An example is shown in the next section.

7. Tip-vortex cavitation

Predicting tip-vortex cavitation has always been a great challenge. It was long believed that cavitation models used in CFD (like the Schnerr-Sauer model used here) are not capable of predicting this type of cavitation. This view was supported by the usual grid-dependence studies that suggested that no significant changes in solution would happen with further refinement because thrust and torque were well converged while the tip-vortex cavitation was limited to a small zone near blade tip.

The tip-vortex cavitation can be visualized by creating an iso-surface of vorticity, as shown in figure 10. By locally refining the grid within this vorticity iso-surface to a sufficiently low level, one can better resolve the extremely high gradients of velocity and pressure across

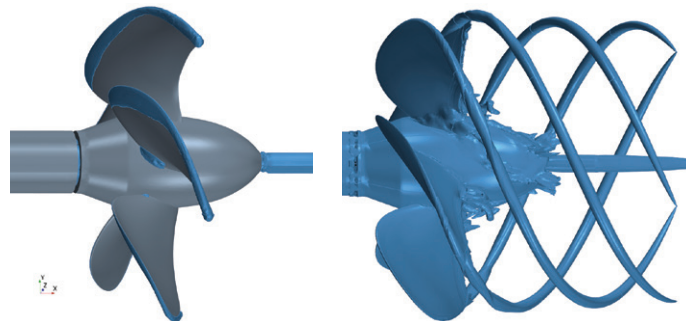


Figure 10. Iso-surfaces of 5 percent vapor volume fraction (left) and of vorticity magnitude (right); computation using Reynolds-averaged Navier-Stokes equations, a version of k- ϵ turbulence model and the Schnerr-Sauer cavitation model.

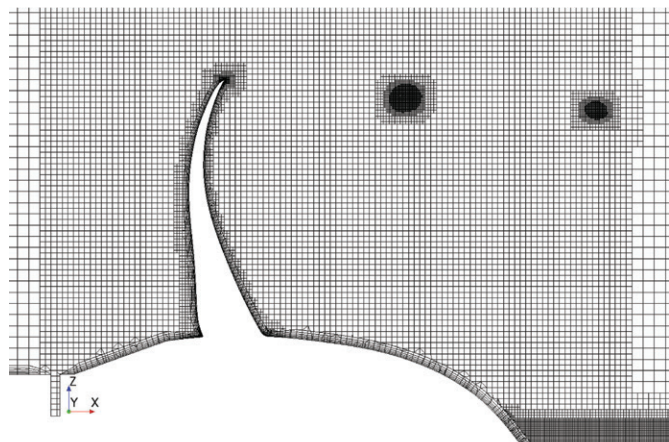


Figure 11. A longitudinal section through the computational grid showing local refinement within the tip vortex zone as indicated by the vorticity iso-surface from figure 10.

the tip vortex. A section through such a locally refined grid is shown in figure 11. For this example of a single blade, with periodic conditions in the circumferential direction, the total number of cells is 4.73 million. The cell size within the tip vortex was 0.234 mm ($D/1068$, where D is the propeller diameter, here 250 mm). The grid is also refined within the hub vortex zone. The flow is from left to right; the setup parameters correspond to case no. 5 on page 2.13 in the report by SVA Potsdam.¹² One finer grid was also created by reducing the cell size everywhere in all directions by a factor of 1.5. This grid had about 17 million cells.

Simulation using the locally refined grid (figure 11) and RANS equations with a version of k- ϵ turbulence model and the Schnerr-Sauer cavitation model is shown in figure 12. This shows an improvement in cavitation prediction compared to the result obtained without local grid refinement (figure 10). The improvement is moderate even when the finest grid with 17 million cells for a single blade is used, as shown in figure 12: The tip-vortex cavitation ends too soon even though the grid was refined to a much longer distance. The thrust is 1.8 percent smaller than in the experiment so it is relatively well predicted. However, the thrust was almost equally well predicted already on the grid without local refinement and cavitation in the tip-vortex zone.

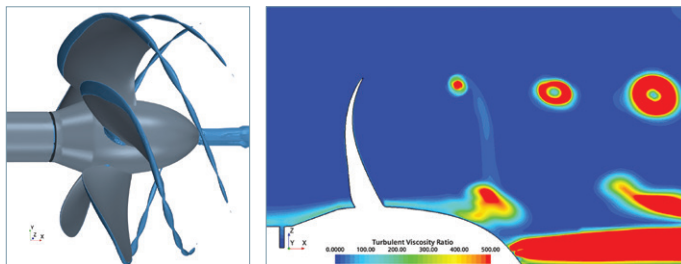


Figure 12. Iso-surfaces of 5 percent vapor volume fraction (left) and contours of turbulent viscosity ratio (right) from a RANS computation of flow around propeller using locally refined grid with 17 million cells for a single blade.

The finest grid is so fine that even an LES approach to turbulence modeling can be used. In this example the wall-adapting local eddy viscosity (WALE) model was used to account for the unresolved part of turbulence,¹⁶ but the grid near the wall was not fine enough to fully resolve the viscous sublayer of the boundary layer on the propeller blades. However, the focus here was to capture the tip-vortex cavitation, and for this the wall treatment is not essential.

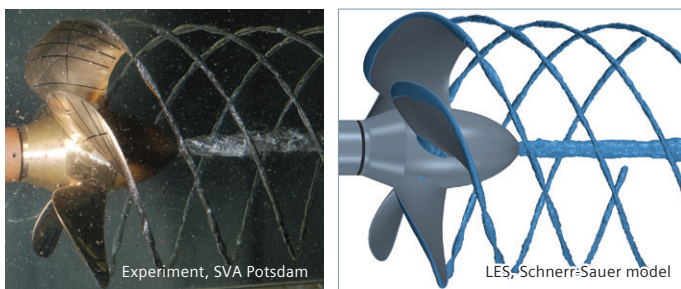


Figure 13. Photograph of tip-vortex cavitation in experiment (left) and iso-surfaces of 5 percent vapor volume fraction (right) from LES computation of flow around propeller using the finest grid with 17 million cells for a single blade.

As can be seen from figure 13, tip-vortex cavitation is very well captured with an LES approach to turbulence. The picture of iso-surface of the vapor volume fraction 0.05 looks similar to the photograph of tip-vortex cavitation taken in experiment.¹³ This shows the turbulence model plays a more important role for the prediction of tip-vortex cavitation than the cavitation model; the simple Schnerr-Sauer model produces a pretty good solution when applied together with LES.

The thrust obtained from the LES-simulation is 4 percent too high; this is probably due to insufficiently fine grid near walls. The DES approach uses a RANS approach in the near wall region for which the current grid was adequate, and LES in zones away from wall. This sounds like a good choice for predicting the flow around a propeller blade. Indeed, the results obtained with Improved Delayed DES,¹⁷ produces the best solution: tip-vortex cavitation extends as far as the grid is fine enough, like in LES, but the thrust is now only 1.5 percent below measured value, which is as good as in RANS solutions. This result also has an adequate resolution of tip-vortex cavitation (see figure 14).

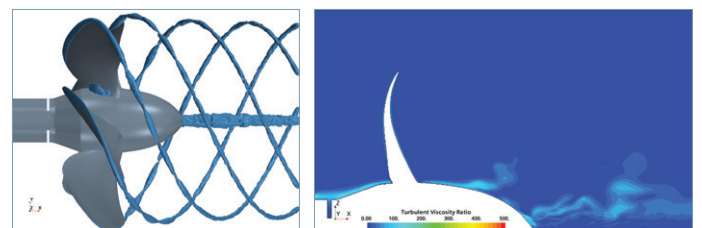


Figure 14. Iso-surfaces of 5 percent vapor volume fraction (left) and contours of turbulent viscosity ratio (right) from a DES computation of flow around the propeller using the finest grid with 17 million cells for a single blade.

The question is why is the turbulence model so important for capturing tip-vortex cavitation? The answer comes from comparing turbulent viscosity ratios (the ratio of turbulent viscosity over fluid viscosity) for the RANS and DES simulations presented in figures 12 and 14. While in DES and LES simulations turbulent viscosity in the tip vortex zone is insignificant, every RANS model produces high turbulent viscosity. This leads to a smearing of velocity gradients, and that in turn leads to an increase in pressure. Once the pressure in the tip-vortex zone becomes higher than saturation level, cavitation stops.

The pressure inside the tip vortex cavitation zone is nearly constant and slightly below saturation pressure, as can be seen from figure 15. However, outside the cavitation zone the pressure increases rapidly, as can be seen from the dense pressure contours around the vortex core. The streamwise velocity component is also almost constant inside the tip vortex, as shown in figure 15, but the gradients with which the velocity decreases on one side and increases on the other side of the vortex core are extremely high. Thus, for a successful resolution of tip-vortex cavitation one needs a fine grid to resolve the extreme pressure and velocity gradients around the tip-vortex core, and a turbulence model that does not generate high turbulent viscosity in this zone in spite of high velocity gradients. The cavitation model seems to play a less important role.

Figure 15 also shows that in a small zone within the hub vortex and close to the blade tip, the absolute pressure is below -1,000 Pa. In fact, the minimum pressure at the suction side near the leading edge is much lower. As discussed previously, this is due to the fact that:

- Pure liquid can sustain tensile stresses due to negative pressure to a relatively high degree
- The bubble growth rate is finite

Thus, where fluid velocity is high and the residence times of bubbles within a low-pressure zone are short, absolute pressure in the liquid can be negative. Some cavitation models cannot account for this behavior, which is sometimes even advertised as a quality feature of the model. However, it is well known that cavitation strongly depends on liquid purity; if all solid particles and dissolved non-condensable gases were removed from water, it would not cavitate until pressure drops to a low level.

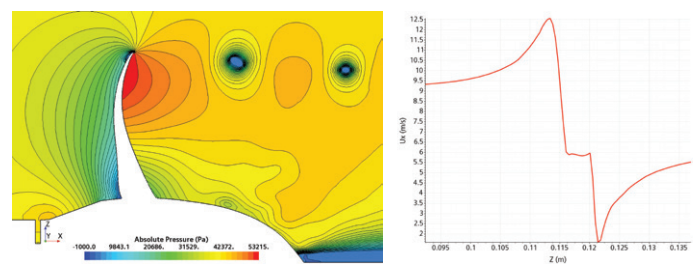


Figure 15. Contours of absolute pressure in a longitudinal section through propeller blade and hub (left) and the profile of streamwise velocity component in radial direction across tip vortex (right) from a DES computation of flow around the propeller using a locally refined grid with 17 million cells for a single blade.

8. Solution-adaptive grid refinement

In many flows, features which need to be resolved change in size and shape over time. It is therefore important to be able to adapt the grid to the changing flow features automatically. Such an example is the growth and collapse of a cavitation bubble near a wall. In the example detailed here, the initial diameter of the bubble was chosen to be 0.26 mm with the bubble center being initially 1.5 mm away from a solid wall. The initial pressure inside the bubble is taken to be 100 bar, while the pressure in the liquid is at the atmospheric level. The bubble is let loose and it expands to a maximum diameter of 2.2 mm.

Simcenter STAR-CCM+ contains an adaptive mesh refinement (AMR) model, which automatically refines (and coarsens) the mesh to capture complex flow features. The refinements are based on the position of the free surface. Here, AMR is set up with a minimum cell size of 3.125 μm . There are four permanent coarsening levels above the background mesh size of 50 μm , as shown in figure 16.

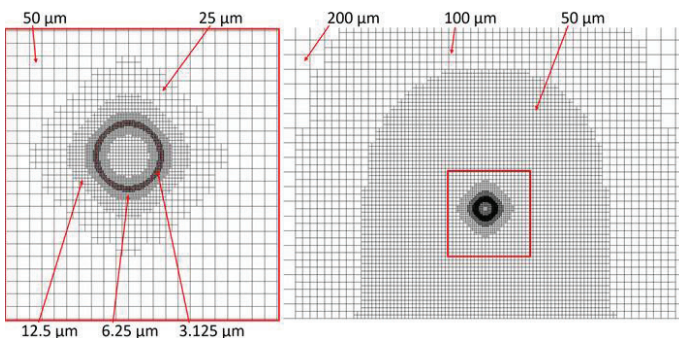


Figure 16. Initial grid for the study of bubble growth and collapse near wall (the refinement within red box is automatically created by AMR based on the initial position of the free surface).

Without AMR, one would need around 500 million cells to achieve the same resolution in the volume over which the interface moves during the growth and collapse process (to cover the maximum bubble diameter

and the distance to the wall). Instead, using AMR, the desired resolution of the interface is ensured at all times, with a gradual coarsening away from the interface and at a much lower total cell count. The number of cells varies during different phases of the process, from just above a million in the early stage (small spherical bubble) to the maximum of around 10 million cells at the time when the bubble has its maximum diameter and in the final stage of bubble collapse. Figure 17 shows the variation of bubble size with time and the related grid at two time instants.

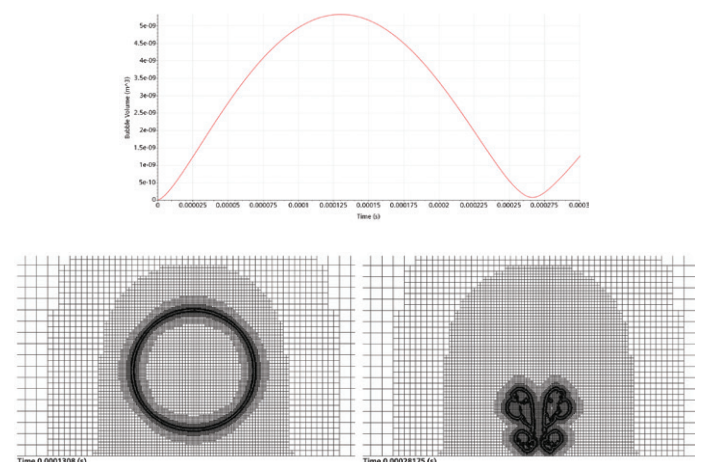


Figure 17. Variation of bubble volume with time (upper) and sections through the grid at two time instants (lower).

During the bubble growth phase, liquid around it is pushed away and the bubble overexpands due to the inertia of liquid. During the collapse phase, liquid flows back toward the interface. Due to the presence of the wall below the bubble, the flow is asymmetric and a liquid jet is formed that penetrates the bubble, making a torus out of it. This jet impinges onto the wall with a high impact velocity of 80 m/s, which is one of the reasons for cavitation erosion. AMR makes such detailed studies possible at a moderate computational cost.

9. Scale effects

Scale effects play an important role in ship hydrodynamics: It is practically impossible to match both Froude and Reynolds numbers in an experiment at model scale and in full scale. The same is true for studies of cavitating flow around a propeller. The model-scale propeller used in experiments is around 40 times smaller than the full-scale propeller, and it rotates much faster. For this reason, cavitation is present on propeller blade during its full rotation in model scale, while at full scale, cavitation is present only during one-third of rotation. See figure 18 for an example of a comparison. As figure 18 shows, the similarity between the flows in model and full scale is limited, making an extrapolation from results obtained in model scale to full scale rather difficult.

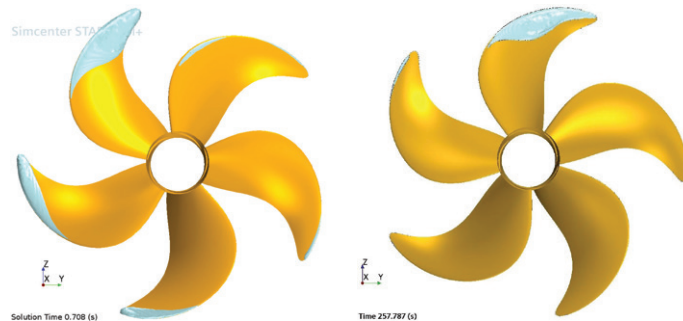


Figure 18. Iso-surfaces of 5 percent vapor volume fraction on propeller blades: model scale (left) and full scale (right).

Another problem with cavitation studies in model scale is that experiments are usually performed in a cavitation tunnel with a relatively small cross-section and without a free surface. This means the boundary conditions in laboratory tests and in full-scale operation are not even

similar. Thus, the flow around the laboratory propeller is different from what it would be if the free surface was present and the blockage effects were negligible. The reflection of pressure waves from cavitation tunnel walls is also problematic, especially if pressure fluctuations on propeller blades, rudder and the hull above the propeller are being studied. Even though experiments are usually trusted as representing the truth, that truth is not the one we need to know, and the measurement data is also affected by errors. It is not unusual that results from different experiments for nominally the same flow differ by as much as the difference between simulation and experiment.

Performing simulation at full scale is no more difficult than at model scale: One only needs to reduce the thickness of the near-wall cells compared to the grid that would be suitable for a simulation at model scale to ensure the same number of cells is present within the logarithmic range of the boundary layer. The far-field boundary conditions are easy to impose, and the effects of free surface waves – both incoming and ship-induced – and ship motion in waves can easily be taken into account.

Although the quality of CFD predictions has been verified in numerous comparisons between simulation and experimental data, confidence in full-scale simulation is still limited. The problem is that full-scale data for comparisons is scarce. In our experience, there is nothing to suggest the accuracy of CFD solutions could be lower at full than at model scale. We hope that more data from full-scale measurements will become available in the near future, and that full-scale simulation and analysis will become commonplace.

Conclusion

This white paper examines important aspects and challenges in simulating cavitating flows, especially flows around a propeller. CFD simulation of cavitation can be highly accurate, indeed more accurate than model-scale experiments. But it is important to understand the potential sources of error, their relative effect on results and how to reduce them as much as possible.

Cavitation on a propeller can be predicted with satisfactory accuracy using common cavitation models provided the grid is locally refined within appropriate zones.

Capturing tip-vortex cavitation requires a turbulence model that does not produce excessive turbulent viscosity. LES and DES models are best, but there are also proposals (such as the Reboud correction)¹⁸ to avoid excessive turbulent viscosity in RANS models, which may be of use.

An accurate representation of the propeller geometry by the computational grid is also vital. It is especially important to resolve the leading edge curvature: insufficient grid resolution here can falsify the geometry and

affect the splitting of the flow to the pressure and suction sides of the propeller blades. Simulation can also be used to study the effects of manufacturing tolerances (the shape of the blades as built compared to the CAD model) on the flow field and propeller performance.

In ship hydrodynamics, one of the most important tasks is to determine hull resistance and to choose a propeller that has the thrust to match the resistance at a minimum required power. With scaling effects undermining the accuracy of extrapolations from model tests and with an increasing body of evidence that full-scale CFD simulations are achieving engineering-level accuracy, the move to simulating full-scale propeller performance under actual operating conditions must become the state-of-the-art method for designing efficient ships. The workshop organized by Lloyds Register in 2016 demonstrated that full-scale simulation of self-propulsion can be reliably conducted with state-of-the-art CFD software¹⁹ and the examples shown in this paper also demonstrate the advantages of full-scale simulation for propellers.

References

1. *Cavitation in control valves*. Technical information, Samson AG, www.samson.de.
2. P. A. Durbin and B. A. Pettersson Reif. *Statistical theory and modeling for turbulent flows* (second edition). Chichester, England: Wiley, 2011.
3. S. B. Pope. *Turbulent flows*. Cambridge: Cambridge University Press, 2000.
4. D. C. Wilcox. *Turbulence modeling for CFD* (third edition). La Cañada, California: DCW Industries, Inc, 2006.
5. F. R. Menter. "Two-equation eddy-viscosity turbulence models for engineering applications." *AIAA J.*, 32, 1598-1605, 1994.
6. J. Smagorinsky. "General circulation experiments with the primitive equations. Part I": The basic experiment. *Monthly Weather Review*, 91, 99-164, 1963.
7. G. H. Schnerr and J. Sauer. "Physical and numerical modeling of unsteady cavitation dynamics." *Fourth international conference on multiphase flow*. New Orleans, Louisiana, United States, 2001.
8. Internal Report, Hamburg Ship Model Basin (HSVA), 1999.
9. S. Muzaferija; D. Papoulias; M. Perić. "VOF simulations of hydrodynamic cavitation using the asymptotic and classical Rayleigh-Plesset models." *Proc. 5th Int. Symp. On Marine Propulsion smp'17*. Espoo, Finland, June 2017.
10. https://www.sva-potsdam.de/wp-content/uploads/2020/11/PPTC-update_on_cavitation-VP1304vsP1790-1-1.pdf
11. S. Jin, R. Zha, H. Peng, W. Qiu and S. Gospodnetic. 2D CFD studies on effects of leading-edge propeller manufacturing defects on cavitation performance. SNAME Maritime Convention 2020 – A Virtual Event, September 29 – October 2, 2020.
12. SVA Report No. 3753, page 2.13, Case No. 5. <https://www.sva-potsdam.de/wp-content/uploads/2016/03/SVA-report-3753.pdf>.
13. SVA Report No. 3753, page 2.9, Case No. 40. <https://www.sva-potsdam.de/wp-content/uploads/2016/03/SVA-report-3753.pdf>.
14. B. De Laage de Meux, B. Audebert, R. Manceau and R. Perrin. "Anisotropic linear forcing for synthetic turbulence generation in large eddy simulation and hybrid RANS/LES modeling." *Physics of Fluids*, 27 (3), 035115, 2015.
15. A. Skillen, A. Revell and T. Craft. "Accuracy and efficiency improvements in synthetic eddy methods." *Int. J. Heat and Fluid Flow*, 62, 386-394, 2016.
16. F. Nicoud and F. Ducros. "Subgrid-scale stress modeling based on the square of the velocity gradient tensor." *Flow, Turbulence and Combustion*, 62, 183-200, 1999.
17. P.R. Spalart, S. Deck, M.L. Shur, K.D. Squires, M. Strelets and A. Travin. "A new version of detached eddy simulation, resistant to ambiguous grid densities.". *Theor. Comput. Fluid Dynamics*, 20, 181-195, 2006.
18. J.L. Reboud; B. Stutz; O. Goutier. "Two-phase flow structure of cavitation: experiment and modeling of unsteady effects." In Proc. *Third Int. Symp. on Cavitation*. Grenoble, France, April 7-10, 1998.
19. D. Ponkratov (Ed.), Proceedings: 2016 Workshop on Ship Scale Hydrodynamic Computer Simulations, Lloyd's Register, Southampton, United Kingdom, 2017.

Siemens Digital Industries Software

Headquarters

Granite Park One
5800 Granite Parkway
Suite 600
Plano, TX 75024
USA
+1 972 987 3000

Americas

Granite Park One
5800 Granite Parkway
Suite 600
Plano, TX 75024
USA
+1 314 264 8499

Europe

Stephenson House
Sir William Siemens Square
Frimley, Camberley
Surrey, GU16 8QD
+44 (0) 1276 413200

Asia-Pacific

Unit 901-902, 9/F
Tower B, Manulife Financial Centre
223-231 Wai Yip Street, Kwun Tong
Kowloon, Hong Kong
+852 2230 3333

About Siemens Digital Industries Software

Siemens Digital Industries Software is driving transformation to enable a digital enterprise where engineering, manufacturing and electronics design meet tomorrow. The Xcelerator™ portfolio, the comprehensive and integrated portfolio of software and services from Siemens Digital Industries Software, helps companies of all sizes create and leverage a comprehensive digital twin that provides organizations with new insights, opportunities and levels of automation to drive innovation. For more information on Siemens Digital Industries Software products and services, visit siemens.com/software or follow us on [LinkedIn](#), [Twitter](#), [Facebook](#) and [Instagram](#). Siemens Digital Industries Software – Where today meets tomorrow.

siemens.com/software

© 2021 Siemens. A list of relevant Siemens trademarks can be found [here](#).

Other trademarks belong to their respective owners.

83381-C4 3/21 H